JOC The Journal of Organic Chemistry

pubs.acs.org/joc Article

Reduction Resistant and Rigid Nitroxide Spin-Labels for DNA and RNA

Haraldur Y. Juliusson and Snorri Th. Sigurdsson*

Cite This: J. Org. Chem. 2020, 85, 4036−4046 Read Online

ABSTRACT: Electron paramagnetic resonance (EPR) spectroscopy, coupled with site-directed spin labeling (SDSL), is a useful method for studying conformational changes of biomolecules in cells. To employ in-cell EPR using nitroxide-based spin labels, the structure of the nitroxides must confer reduction resistance to withstand the reductive environment within cells. Here, we report the synthesis of two new spin labels, **EÇ** and **EÇm**, both of which possess the rigidity and the reduction resistance needed for extracting detailed structural information by EPR spectroscopy. **EÇ** and **EÇm** were incorporated into DNA and RNA, respectively, by oligonucleotide synthesis. Both labels were shown to be nonperturbing of the duplex structure. The partial reduction of **EÇm** during RNA synthesis was circumvented by the protection of the nitroxide as a benzoylated hydroxylamine.

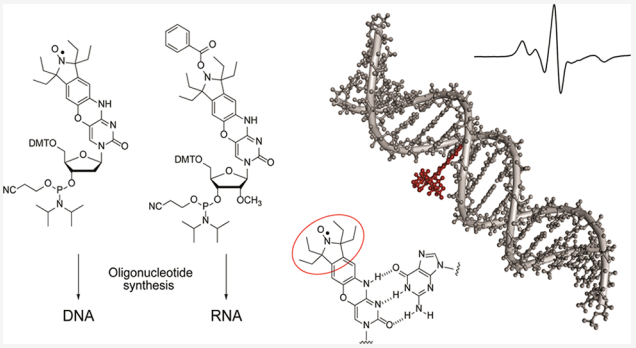

INTRODUCTION

Nucleic acids are central to molecular biology and partake in essential biological processes,[1] including storage, expression, and transmission of genetic information,[2] as well as catalysis of chemical reactions[3,4] and regulation of genetic expression.[5−7] Understanding their biological functions relies on structural knowledge. Biomolecules have been intensively studied in vitro by a number of biochemical and biophysical methods, such as X-ray crystallography,[8] nuclear magnetic resonance (NMR) spectroscopy,[9,10] Förster resonance energy transfer (FRET),[11,12] and electron paramagnetic resonance (EPR) spectroscopy.[13−16] Although biomolecules have been extensively studied in vitro, the question remains whether the structure and dynamics of biomolecules are different in cells, since the intracellular environment may be impossible to reproduce in vitro, in particular factors such as viscosity, molecular crowding, interactions with other macromolecules, and concentration of ions.[17]

An increased effort is being directed toward exploring biomolecules within cells, in particular using spectroscopic methods, such as NMR, FRET, and EPR.[17−20] In-cell NMR has been used to study the structure and dynamics of nucleic acids in several cell types, along with membranes and disordered proteins.[17,19−23] In-cell NMR has mostly been used to monitor enzymatic or "nonspecific" interactions[21] and requires isotopic labeling of molecules to overcome cellular background signals. In-cell FRET has been used to study inter- and intramolecular interactions through distance measurements between two fluorescent tags.[24,25] EPR spectroscopy has also been used to measure distances within biomolecules in cells, and recent studies have highlighted its advantages.[18,26,27] EPR requires small amounts of materials, has virtually no background signals, is not limited by molecular size, and structural information can be readily obtained through distance measurements by dipolar EPR experiments, such as pulsed electron-electron double resonance (PELDOR/DEER).[26,28−30]

There are examples of paramagnetic biomolecules, such as metalloproteins[31] and proteins, that contain paramagnetic cofactors.[32] However, the majority of biomolecules are diamagnetic, and, therefore, a paramagnetic center (spin label) must be introduced to carry out EPR studies. For in-cell EPR, three types of spin labels have been used. Gd(III) complexes have been used for distance measurements in proteins (Figure 1A),[33−35] for example, ubiquitin that contained two 4PS-PyMTA-Gd(III) labels. Trityl radicals (Figure 1B) have also been used for distance measurements in cells, specifically between a trityl-labeled cytochrome P450 and a native metal cofactor.[36] Nitroxides have also been used for in-cell EPR,[18,26−30,37,38] but the limitation of most nitroxides is that they are rapidly reduced in the reducing environment encountered within cells.[37,39,40] However, steri-

Received: November 4, 2019
Published: February 27, 2020

https://dx.doi.org/10.1021/acs.joc.9b02988
J. Org. Chem. 2020, 85, 4036−4046

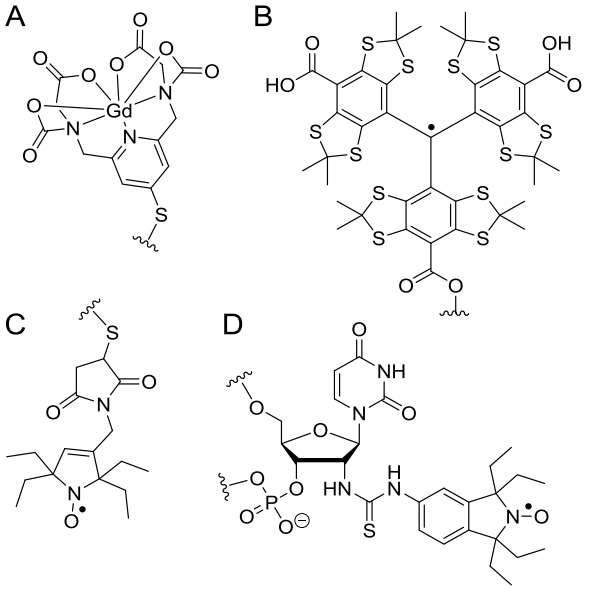

Figure 1. Different spin labels used for in-cell EPR measurements. (A) 4PS-PyMTA-Gd(III) linked to a protein.[43] (B) Trityl-based spin label linked to a protein.[36] (C) M-TETPO linked to a protein.[41] (D) Tetraethyl-derived spin label conjugated to a 2′-amino labeled uridine through a thiourea linkage.[42]

cally shielded nitroxides, in particular, tetraethyl-derived nitroxides, are resistant toward reduction.[40] For example, a tetraethyl-derived pyrrolidine nitroxide has been used to spin label a chaperone protein for in-cell EPR (Figure 1C). Only minimal reduction of the radical was observed and enabled the EPR study of structural features of the chaperone protein through the determination of interspin distances.[41] A tetraethyl-derived isoindoline spin label has recently been used for post-synthetic labeling of 2′-amino groups of RNA (Figure 1D) and shown to be stable in the presence of ascorbic acid.[42] Preliminary in-cell EPR measurements with this label have revealed structural changes in duplex RNAs (unpublished data). However, the semiflexible nature of the linker attaching the spin label to the RNA limited the structural information that could be obtained.

The rigid spin labels **Ç**[44] and **Çm**[45] (Figure 2) have been shown to provide more detailed information on structural changes and dynamics in nucleic acids[46] than flexible and semiflexible labels. Here, we describe the synthesis and characterization of the corresponding tetraethyl nitroxide spin labels **EÇ** and **EÇm** (Figure 2). These spin labels

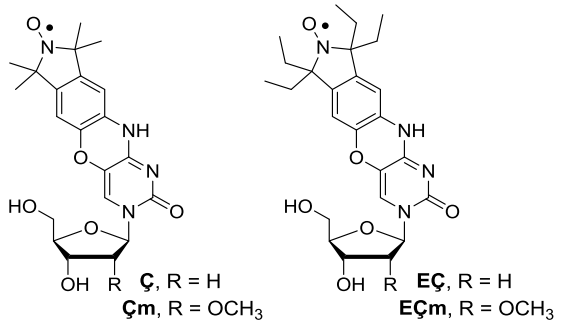

Figure 2. Rigid spin labels **Ç**[44] and **Çm**[45] and their corresponding tetraethyl derivatives **EÇ** and **EÇm**.

combine two characteristics necessary for obtaining detailed structural information about nucleic acids in cells by EPR spectroscopy, namely, rigidity and reduction resistance.

RESULTS AND DISCUSSION

Synthesis of EÇ and EÇm and Their Stability Toward Reduction. The synthesis of **EÇ** and **EÇm** started with the preparation of ethylisoindoline derivative **4** (Scheme 1).

Scheme 1. Synthesis of Tetraethylisoindoline 4

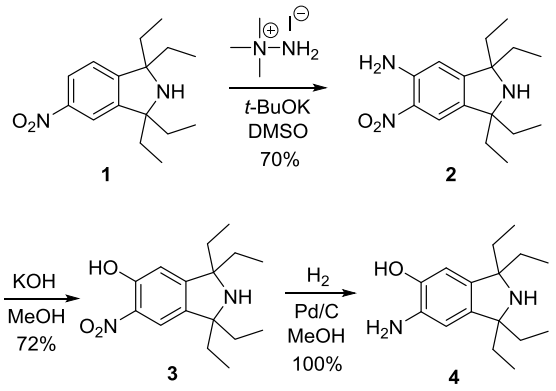

Compound **1**[47] was aminated[48] to afford amino-nitro derivative **2**. The hydrolysis of **2** yielded **3**, and hydrogenation of the nitro group gave ethylisoindoline-derived aminophenol **4**. To incorporate the ethylisoindoline moiety into nucleosides, the dihalogenated nucleosides **5**[44] and **6**[45] were coupled with **4** in the presence of Et_3N to provide intermediates **7** and **8**, respectively, followed by ring closure[44,45,49] to afford phenoxazine derivatives **EÇf** and **EÇmf**. Direct oxidation of **EÇf** and **EÇmf** using either hydrogen peroxide and Na_2WO_4[44] or *m*-chloroperoxybenzoic acid (*m*-CPBA)[50] under a variety of conditions resulted in very low yields of the desired product along with multiple other products. However, oxidation of TBDMS-protected **EÇf** and **EÇfm** with *m*-CPBA in the presence of NaN_3[48] afforded **9** and **10** in excellent yields. The TBDMS groups were subsequently removed with tetrabutylammonium fluoride (TBAF) to yield nucleosides **EÇ** and **EÇm**.

The resistance of **EÇm** toward reduction in the presence of ascorbic acid, frequently used to evaluate the stability of nitroxides,[40] was investigated and compared to its tetramethyl derivative **Çm**.[45] The normalized EPR signal intensity was plotted as a function of time and showed that the tetramethyl derived **Çm** was almost fully reduced within 1 h, while ca. 90% of the **EÇm** nucleoside was still intact after 16 h (Figure S29).

The 5′-hydroxyl groups of **EÇ** and **EÇm** were protected as 4,4′-dimethoxytrityl (DMT) ethers and subsequent 3′-phosphitylation yielded phosphoramidites **11** and **12** (Scheme 2), used for incorporation of **EÇ** and **EÇm** into DNA and RNA oligonucleotides by solid-phase synthesis, respectively. While working with DMT-protected **EÇ**, **EÇm** and phosphoramidites **11** and **12**, we discovered that the DMT groups were unusually labile. Even dissolving these compounds in polar and/or protic solvents, such as CH_3CN or MeOH, leads to a rapid loss of the DMT group. The use of nonpolar or chlorinated solvents such as CH_2Cl_2 or 1,2-dichloroethane circumvented this decomposition.

Syntheses of Spin-Labeled DNA Oligonucleotides. Phosphoramidite **11** was used for the synthesis of seven

https://dx.doi.org/10.1021/acs.joc.9b02988
J. Org. Chem. 2020, 85, 4036−4046

Scheme 2. Synthesis of Spin-Labeled Nucleosides EÇ and EÇm and Their Corresponding Phosphoramidites[a]

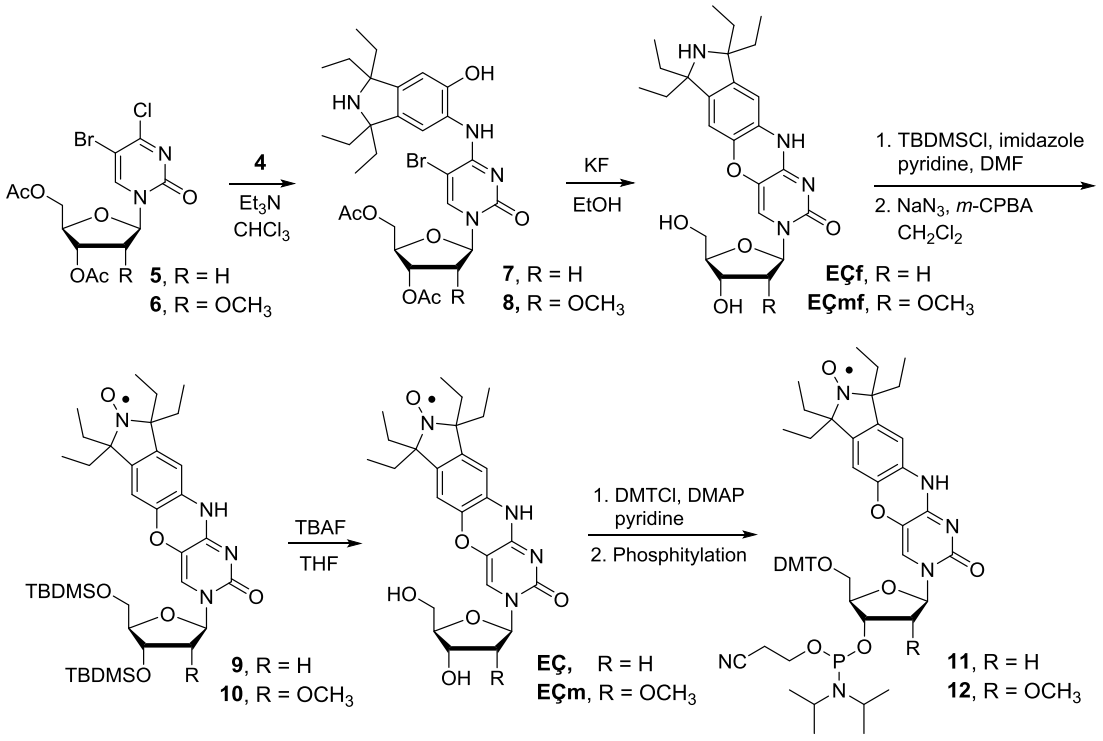

[a]Yields were as follows: **EÇf** (56%, over 2 steps), **EÇmf** (60%, over 2 steps), **9** (83%, over 2 steps), **10** (81%, over 2 steps), **EÇ** (91%), **EÇm** (94%), **11** (77%, over 2 steps), and **12** (63%, over 2 steps).

different oligodeoxynucleotides containing **EÇ** by automated solid-phase synthesis (Table S1). The DNAs varied in length and position of the spin label. The spin-labeled phosphoramidite **11** coupled well during the solid-phase synthesis, as indicated by a strong orange color of the trityl cation that appears during the removal of the DMT group. The analysis of the crude oligodeoxynucleotides by denaturing polyacrylamide gel electrophoresis (DPAGE) did not reveal any failure bands that would have resulted in a partial coupling of **11**. The **EÇ**-modified oligomers migrated slightly slower than the unmodified strands of the same sequence by DPAGE, consistent with the incorporation of the spin label, which was confirmed by mass spectrometry (Table S1).

The DNA oligomers were enzymatically digested, and the digests were analyzed by high-performance liquid chromatography (HPLC) (Figure S30).[51,52] The HPLC chromatograms for digests of DNAs **I**–**VII** each showed five peaks, one for each natural nucleoside and a strongly retained nucleoside that was shown by co-injection[44] to be **EÇ**. Chromatograms for the longer oligonucleotides (**III**, **IV**, **VI**, and **VII**) also contained an additional small peak around 20.5 min that was shown by co-injection to be **EÇf**. It is well-known that nitroxide radicals get partially,[52] or even fully,[53] reduced during oligonucleotide synthesis using the phosphoramidite approach. Although the tetraethyl groups on **EÇ** render the nitroxide significantly more resistant to reduction by common reducing agents, they do not provide full protection against reduction (through disproportionation)[54] by the acids used for oligonucleotide synthesis, dichloroacetic acid and ethylthiotetrazole. The amount of **EÇf** and **EÇ** was quantified, showing that ca. 6–18% of the spin labels had been reduced. These results were further confirmed with spin-counting of DNAs **I**–**VII** by EPR spectroscopy giving 81–100% spin labeling (Table S1). It should be noted that more extensive reduction was observed in oligodeoxynucleotides of similar length that were synthesized using the phosphoramidite of the tetramethyl derived **Ç**.[52]

A molecular model of a **EÇ** within a B-form DNA duplex (Figure 3A) shows that the spin label is well accommodated in the major groove of the duplex. To determine experimentally whether the **EÇ** spin label caused a structural perturbation of the B-DNA, circular dichroism (CD) spectra were recorded (Figure S32), along with collecting thermal denaturation data (Table 1 and Figure S33). The CD spectra of the modified and

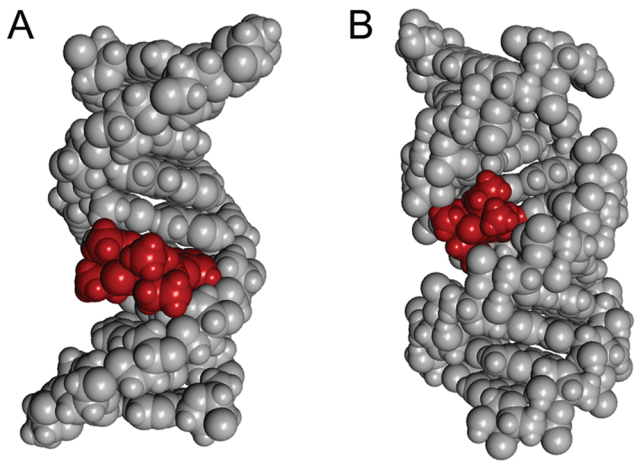

Figure 3. Space-filling models of **EÇ**- and **EÇm**-labeled oligonucleotide duplexes. (A) B-form DNA duplex with **EÇ** projected into the major groove. (B) A-form RNA duplex containing **EÇm**. The oligonucleotide constituents are shown in gray and the spin-labeled nucleotides in red.

https://dx.doi.org/10.1021/acs.joc.9b02988
J. Org. Chem. 2020, 85, 4036–4046

Table 1. Sequences of Spin-Labeled DNA and RNA Duplexes and Their Thermal Denaturation Analysis

	DNA and RNA sequences	T_M (°C)	ΔT_M
A	5′-d(CGCGAATTCGCG)-3′ 3′-d(GCGCTTAAGCGC)-5′	58.2	
B	5′-d(CGCG AATTEÇGCG)-3′ 3′-d(GCGEÇTTAAG CGC)-5′	63.8	+5.6
C	5′-d(GACCTCGCATCGTG)-3′ 3′-d(CTGGAGCGTAGCAC)-5′	60.8	
D	5′-d(GACCTCGEÇATCGTG)-3′ 3′-d(CTGGAGCG TAGCAC)-5′	59.3	−1.5
E	5′-d(AGTGGACGCTTGGGGTGTA)-3′ 3′-d(CACCTGCGAACCCCACATA)-5′	66.6	
F	5′-d(AGTGGAEÇGCTTGGG GTGTA)-3′ 3′-d(CACCTG CGAACCCEÇACATA)-5′	63.8	−2.8
G	5′-d(AGTGGAEÇGCTTGG GGTGTA)-3′ 3′-d(CACCTG CGAACCEÇCACATA)-5′	65.0	−1.6
H	5′-d(AGTGGAEÇGCTTG GGGTGTA)-3′ 3′-d(CACCT GCGAACEÇCCACATA)-5′	65.8	−0.8
I	5′-d(AGTGGAEÇGCTT GGGGTGTA)-3′ 3′-d(CACCT GCGAAEÇCCCACATA)-5′	67.4	+0.8
J	5′- AGUGGACGCUUGUGGGGUGUA -3′ 3′- CACCUGCGAACACCCCACAUA-5′	77.0	
K	5′- AGUGGAEÇmGCUUGUGGGG UGUA -3′ 3′- CACCUG CGAACACCCEÇmACAUA-5′	74.0	−3.0
L	5′- AGUGGAEÇmGCUUGUGGG GUGUA -3′ 3′- CACCUG CGAACACCEÇmCACAUA-5′	76.0	−1.1
M	5′- AGUGGAEÇmGCUUGUGG GGUGUA -3′ 3′- CACCUG CGAACACEÇmCCACAUA-5′	75.6	−1.4
N	5′- AGUGGAEÇmGCUUGUG GGGUGUA -3′ 3′- CACCUG CGAACAEÇmCCCACAUA-5′	74.6	−2.4

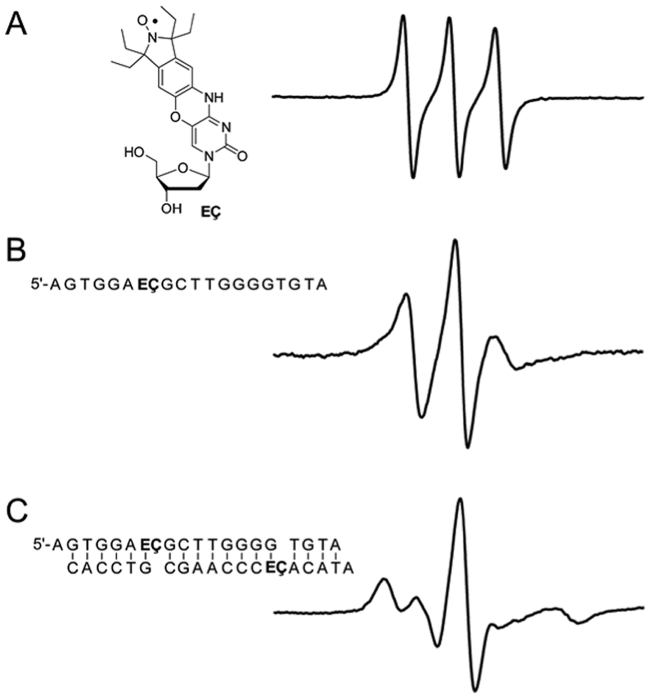

Figure 4. (A) EPR spectrum of **EÇ**. (B) EPR spectrum of a **EÇ**-labeled 19-mer DNA single-strand 5′-d-(AGTGGA**EÇ**GCTTGGGGTGTA)-3′. (C) EPR spectrum of a **EÇ**-labeled duplex 5′-d(AGTGGA**EÇ**GCTTGGGGTGTA)-3′·5′-d-(ATACA**EÇ**CCCAAGCGTCCAC)-3′. EPR spectra were recorded at 20 °C in a phosphate buffer (2 nmol of DNA; 10 mM phosphate, 100 mM NaCl, 0.1 mM Na_2EDTA, pH 7.0).

unmodified DNA duplexes were almost identical, all possessing negative and positive molar ellipticities at ca. 250 and 280 nm, respectively, characteristic of a right-handed B-DNA. In general, the thermal denaturation experiments showed that the spin labels did not result in a significant decrease in the melting temperature, with ΔT_Ms ranging from −0.8 to −2.8 °C. The increased stability was actually observed for duplexes **B** and **I**. The increase of the T_M for duplex **B** of +5.6 °C and the decrease for duplex **D** of −1.5 °C are nearly identical to what has been observed for **Ç** in the same location of the same sequence (ΔT_M +5.7 °C and ΔT_M −1.1 °C, respectively).[51]

All oligonucleotides were characterized by continuous-wave (CW) EPR spectroscopy (Figure S34), which also confirmed duplex formation. Figure 4 shows a comparison of the CW−EPR spectra of **EÇ**, the **EÇ**-labeled 19-mer DNA single-strand **III**, and the corresponding 19-mer DNA duplex **F**. The nucleoside showed three sharp lines (Figure 4A) that broadened after incorporation into the 19-mer oligoribonucleotide 5′-d(AGTGGA**EÇ**GCTTGGGGTGTA)-3′ (Figure 4B). Upon annealing to its complementary strand 5′-d(ATACA**EÇ**CCCAAGCGTCCAC)-3′, the CW−EPR spectrum broadened further, showing a splitting of the high- and low-field components (Figure 4C), characteristic for the formation of a spin-labeled duplex containing a rigid spin label.[44,45]

Syntheses of Spin-Labeled RNA Oligonucleotides. In a manner analogous to the synthesis of **EÇ**-modified DNA, phosphoramidite **12** was used to synthesize five 21-nucleotide long **EÇm**-labeled RNAs (Table S1). HPLC chromatograms of enzymatic digests of RNAs **XII**−**XVI** (Figure S31A−E) showed five peaks, one for each natural nucleoside and one for **EÇm**. An additional peak or two were observed in digests of five oligonucleotides, one corresponding to inosine (from a partial enzymatic hydrolysis of A by an adenosine deaminase contamination in phosphodiesterase I)[55] (Figure S31B−E) and the other corresponding to **EÇmf** (Figure S31A,B,D). The reduction of **EÇm** to **EÇmf** was determined from the chromatograms to be 30−49% and further confirmed by spin counting using EPR spectroscopy (Table S1, **XII**, **XIII**, and **XV**). The more extensive reduction of **EÇm** compared to reduction of **EÇ** during DNA synthesis can be explained by longer exposure of the spin label to oligonucleotide reagents during RNA synthesis. Recent reports of protecting nitroxides prior to the oligonucleotide synthesis of RNA have shown to be effective to circumvent their reduction;[52,56] we chose to employ benzoyl protection of the corresponding hydroxylamine of **EÇm**.[52]

Synthesis of Bz-EÇm and Its Corresponding Phosphoramidite. The synthesis of **Bz-EÇm** (Scheme 3) began with reduction of the TBDMS-protected nitroxide **10** to yield the corresponding hydroxylamine, which was subsequently benzoylated to give **13**. Heating **10** at 60 °C for 24 h with 20 equivalents of ascorbic acid was required for reducing this structurally hindered nitroxide. The subsequent removal of the TBDMS groups of **13** gave **Bz-EÇm**. The benzoyl-protecting group was shown to be stable under all conditions used for oligonucleotide synthesis for more than a week (data not shown) and was efficiently removed in 2.5 h using conventional deprotecting conditions for RNA (1:1, 40% $MeNH_2$/40% NH_3 in H_2O), returning **EÇm** in quantitative yields. The 5′-hydroxyl group of **Bz-EÇm** (Scheme 3) was protected as

https://dx.doi.org/10.1021/acs.joc.9b02988
J. Org. Chem. 2020, 85, 4036−4046

Scheme 3. Synthesis of Bz-EÇm and Its Corresponding Phosphoramidite

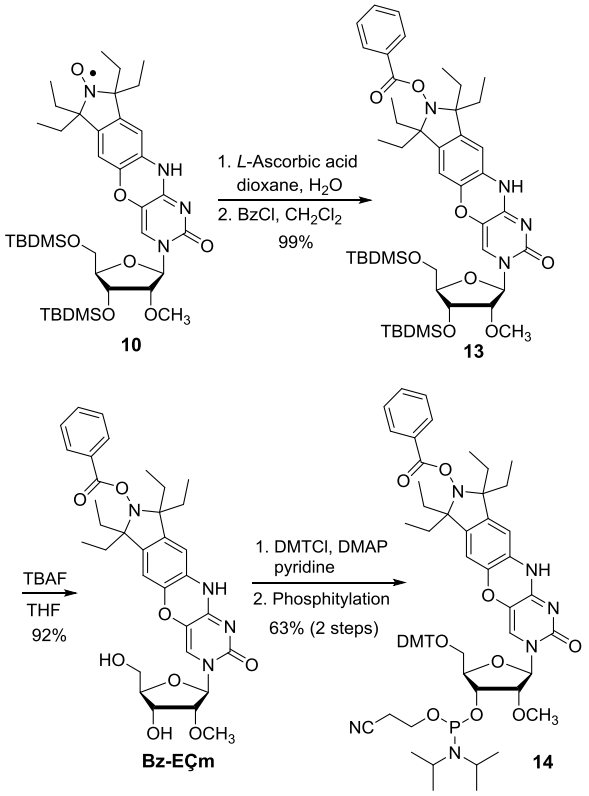

4,4′-dimethoxytrityl (DMT) ether and subsequently phosphitylated to give phosphoramidite **14** in good yields.

Syntheses of Spin-Labeled RNA Oligonucleotides Using Phosphoramidite 14. Phosphoramidite **14** was used to repeat the synthesis of oligonucleotides **XII**, **XIII**, and **XV** (Table S1). As before, the protected spin label coupled well during the solid-phase synthesis. Spin counting by EPR spectroscopy showed 96−99% spin labeling, indicating that little or no reduction of the spin label had occurred during the synthesis (Table S1, **XVII**, **XVIII**, and **XIX**). This was further confirmed by the HPLC analysis of the enzymatic digests of RNAs **XVII**, **XVIII**, and **XIX** (Figure S31F,G,H) that showed the complete absence of **EÇmf**. The HPLC analyses also showed that the benzoyl-protecting group had been completely removed during the RNA deprotection. The stabilities of the spin-labeled duplexes **V**, **XIV** and the **Ç**-labeled DNA 5′-PHO-d(TGAGGTAGTAGGTTGTATAÇT)-3′ were tested in the presence of ascorbic acid, like before with the nucleosides. Figure 5 shows the EPR signal as a function of time. There was a striking difference in the stability of the tetraethyl-derived spin-labeled oligonucleotides as compared to the tetramethyl-derived spin labels: **Ç**-labeled DNA was fully reduced within 20 min, while the tetraethyl-labeled DNA(**EÇ**) and RNA-(**EÇm**) were almost completely intact after 12 h.

A model of **EÇm** within an A-form RNA duplex (Figure 3B) shows that the spin label fits tightly into the major groove of the duplex. CD spectra of the RNA duplexes (unmodified and modified) showed negative and positive molar ellipticities at ca. 210 and 263 nm, respectively, as expected for A-form RNA (Figure S32). Thermal denaturing experiments showed only minor destabilization of the duplexes by **EÇm**, with the ΔT_Ms ranging from −1.1 to −3.0 °C. Since each duplex contains two

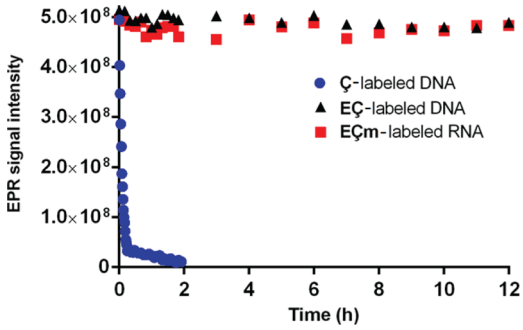

Figure 5. Stabilities of **EÇ**-labeled DNA single-strand **V** (square), **EÇm**-labeled RNA single-strand **XIV** (triangle), and the **Ç**-labeled DNA 5′-PHO-d(TGAGGTAGTAGGTTGTATAÇT)-3′ (circle) toward reduction (5 mM ascorbic acid, 10 mM phosphate, 100 mM NaCl, 0.1 mM Na2EDTA, pH 7.0). PHO is a phosphate.

labels, the change in T_m caused by **EÇm** was less than −2.0 °C per modification, relative to the unmodified RNA, which is a similar result to that obtained with **Çm**-modified RNA duplexes of similar length.[45] All of these RNA duplexes have one strand in common (Table S1, **XVII**), which is complementary to all of the other strands (Table S1, **XVIII**, **XIV**, **XIX**, and **XVI**). Thus, the only difference between the spin-labeled duplexes is the position of **EÇm** in the complementary strand. Therefore, the minor differences in the melting temperatures are likely due to flanking-sequence dependence, as has been observed with both phenoxazine-derived spin labels[45,51] and fluorophores[57,58] in DNA.

CONCLUSIONS

The tetraethyl-derived rigid spin labels **EÇ** and **EÇm** were synthesized and incorporated into DNA and RNA, respectively. The spin-labeled oligonucleotides were analyzed by UV−vis, CD, and EPR spectroscopy as well as enzymatic digestion followed by HPLC analysis. Together this data verified incorporation of the spin labels and showed them to be nonperturbating of duplex structures. A minor reduction of the **EÇ** spin label was observed during the automated synthesis of **EÇ**-labeled DNA, but a substantial reduction of **EÇm** took place during the synthesis of **EÇm**-labeled RNA. This reduction was circumvented by using a benzoyl-protecting group for the hydroxylamine prepared from **EÇm**.[52] The new tetraethyl-derived rigid labels **EÇ** and **EÇm** showed dramatically increased resistance toward reduction by ascorbic acid, when compared to its tetramethyl derivatives **Ç**[44] and **Çm**,[45] which will enable the investigation of structure and dynamics of DNA and RNA by in-cell EPR spectroscopy.

EXPERIMENTAL SECTION

General Materials, Instruments, and Methods. All commercially available reagents were purchased from Sigma-Aldrich co GMBH. or Acros Organics and used without further purification, except diisopropylammonium tetrazolide and 2-cyanoethyl *N,N,N′,N′*- tetraisopropylphosphorodiamidite, which were purchased from ChemGenes Corp. All commercial phosphoramidites, CPG columns, and solutions for oligonucleotide syntheses were also purchased from ChemGenes Corp. 2′-Deoxyuridine and 2′-*O*-methyluridine were purchased from Rasayan Inc. CH_2Cl_2, pyridine, and CH_3CN were dried over calcium hydride and freshly distilled before use. All moisture- and air-sensitive reactions were carried out in oven-dried glassware under an inert atmosphere of Ar. Thin-layer chromatography (TLC) was performed using glass plates precoated with silica gel (0.25 mm, F-25, Silicycle), and compounds were

https://dx.doi.org/10.1021/acs.joc.9b02988
J. Org. Chem. 2020, 85, 4036−4046

visualized under UV light and by *p*-anisaldehyde staining. Column chromatography was performed using 230−400 mesh silica gel (Silicycle). ^{1}H-, ^{13}C- and ^{31}P NMR spectra were recorded with a Bruker Avance 400 MHz spectrometer. Commercial-grade $CDCl_3$ was passed over basic alumina shortly before dissolving tritylated nucleosides for NMR analysis. Chemical shifts are reported in parts per million (ppm) relative to the partially deuterated NMR solvents $CDCl_3$ (7.26 ppm for ^{1}H NMR and 77.16 ppm for ^{13}C), CD_3OD (3.35, 4.78 ppm for ^{1}H NMR and 49.3 ppm for ^{13}C), and dimethyl sulfoxide (DMSO)-d_6 (2.49 ppm for ^{1}H NMR and 39.7 ppm for ^{13}C). ^{31}P NMR chemical shifts are reported relative to 85% H_3PO_4 (at 0.0 ppm) as an external standard. All coupling constants are reported in hertz (Hz). Nitroxide radicals show broadening and loss of NMR signals due to their paramagnetic nature and, therefore, those NMR spectra are not shown. Mass spectrometric analyses of all organic compounds were performed on an high resolution electrospray ionization mass spectrometry (ESI-HRMS) (Bruker, MicrOTOF-Q) in a positive ion mode. DNA and RNA solid-phase oligonucleotide syntheses were performed on an automated ASM800 DNA/RNA synthesizer (BIOSSET Ltd., Russia) using phosphoramidite chemistry. Unmodified and spin-labeled oligonucleotides were synthesized using a trityl-off protocol and phosphoramidites with standard protecting groups on a 1 μmol scale (1000 Å CPG columns). Oxidation was performed with *tert*-butylhydroperoxide (1.0 M) in toluene. Capping and detritylation were performed using standard conditions for DNA and RNA syntheses. Concentrations of the oligonucleotides were determined by measuring UV absorbance at 260 nm using a PerkinElmer Inc. Lambda 25 UV/Vis spectrometer and calculated by Beer's law. Mass spectrometric analyses of **EÇ**- and **EÇm**-labeled oligonucleotides were performed on an ESI-HRMS (Bruker, MicrOTOF-Q) in a negative ion mode. HPLC analyses of enzymatic digests were performed on a Beckman Coulter Gold HPLC system using a Beckman Coulter Ultrasphere C18 4.6 × 250 mm^2 analytical column with UV detection at 254 nm. Solvent gradients for analytical RP-HPLC were run at 1.0 mL/min using the following gradient program: solvent A, triethylammonium acetate (TEAA) buffer (50 mM, pH 7.0); solvent B, CH_3CN; 0−4 min isocratic 4% B, 4−14 min linear gradient 4−20% B, 14−24 min linear gradient 20−50% B, 24−29 min linear gradient 50−80% B, 29−30 min isocratic 80%, 30−35 min linear gradient 80−4% B, and 35−45 min isocratic 4% B. CD spectra of the duplexes were recorded in a Jasco J-810 spectropolarimeter. Cuvettes with 1 mm path length were used, and the CD data were recorded from 350 to 200 nm at 25 °C. Prior to analysis by CD, thermal denaturation, and EPR, an appropriate quantity of each DNA or RNA stock solutions was dried on a Thermo Scientific ISS 110 SpeedVac and dissolved in phosphate buffer (10 mM phosphate, 100 mM NaCl, 0.1 mM Na_2EDTA, pH 7.0). DNA and RNA duplexes were formed by annealing in an MJ Research PTC 200 thermal cycler using the following protocol: 90 °C for 2 min, 60 °C for 5 min, 50 °C for 5 min, 40 °C for 5 min, and 22 °C for 15 min. CW−EPR spectra were recorded on a MiniScope MS200 spectrometer using 100 kHz modulation frequency, 1.0 G modulation amplitude, and 2.0 mW microwave power. The samples were placed in a quartz capillary (BLAUBRAND intraMARK) prior to EPR measurements.

*1,1,3,3-Tetraethyl-6-nitroisoindolin-5-amine (**2**).* To a solution of *N*,*N*,*N*-trimethylhydrazine iodide (1.83 g, 99.9 mmol) in DMSO (15 mL) was added *t*-BuOK (1.12 g, 99.9 mmol), and the solution was stirred at 22 °C for 30 min. Compound **1** (1.00 g, 45.4 mmol) was added, and the solution was stirred further for 14 h. The reaction mixture was poured into ice-cold water (50 mL), followed by extraction with CH_2Cl_2 (3 × 50 mL), and the combined organic phases were dried over Na_2SO_4, filtered, and concentrated in vacuo. The crude product was purified by flash-column chromatography, using a gradient elution (100:0 to 90:10, CH_2Cl_2/MeOH), to give compound **2** (0.750 g, 70%) as an orange solid. ^{1}H NMR (400 MHz, DMSO-d_6) δ 7.62 (s, 1H), 7.29 (s, 2H), 6.73 (s, 1H), 1.56 (qdd, J = 13.8, 7.3, 4.2 Hz, 8H), 0.80 (q, J = 7.6 Hz, 12H) ppm. ^{13}C{^{1}H} NMR (101 MHz, DMSO-d_6) δ 157.0, 146.0, 136.2, 130.0, 118.1, 111.5, 67.3, 66.5, 40.1, 39.9, 39.7, 39.5, 39.3, 39.0, 38.8, 33.3, 33.0, 8.8, 8.7, 8.6 ppm. HRMS (ESI-TOF) m/z: [M + H]$^+$ calcd for $C_{16}H_{26}N_3O_2^+$: 292.2020; found 292.2017.

*1,1,3,3-Tetraethyl-6-nitroisoindolin-5-ol (**3**).* To a solution of potassium hydroxide (13.1 g, 0.234 mmol) in 10% H_2O/MeOH (80 mL) was added 1,1,3,3-tetraethyl-6-nitroisoindolin-5-amine (**2**) (2.75 g, 11.7 mmol), and the reaction mixture heated in a closed vial at 140 °C for 24 h. The reaction mixture was poured onto ice and extracted with EtOAc (3 × 100 mL); the combined organic phases were dried over Na_2SO_4 and the solvent was removed in vacuo. The residue was purified by flash-column chromatography, using a gradient elution (100:0 to 90:10, CH_2Cl_2/MeOH), to give compound **3** (2.01 g, 72%) as a bright yellow solid. ^{1}H NMR (400 MHz, $CDCl_3$) δ 10.69 (s, 1H), 7.77 (s, 1H), 6.82 (s, 1H), 1.76−1.59 (m, 8H), 0.89 (t, J = 7.5 Hz, 12H) ppm. ^{13}C{^{1}H} NMR (101 MHz, $CDCl_3$) δ 155.1, 133.0, 118.5, 113.1, 33.62, 33.43, 29.7, 8.78, 8.73 ppm. HRMS (ESI-TOF) m/z: [M + H]$^+$ calcd for $C_{16}H_{25}N_2O_3^+$: 293.1860; found 293.1878.

*6-Amino-1,1,3,3-tetraethylisoindolin-5-ol (**4**).* A solution of compound **3** (400 mg, 2.54 mmol) in MeOH (30 mL) containing 10% Pd/C (40.0 mg) was stirred in the dark under an atmosphere of H_2 (1 atm) for 2 h. The reaction mixture was filtered through a pad of celite, and the filtrate was concentrated in vacuo to yield crude product **4** (348 mg), which was directly used for the next step without further purification. ^{1}H NMR (400 MHz, $CDCl_3$) δ 6.48 (s, 2H), 1.83−1.49 (m, 8H), 1.07−0.59 (m, 12H). HRMS (ESI-TOF) m/z: [M + H]$^+$ calcd for $C_{16}H_{27}N_2O^+$: 263.2118; found 263.2111.

*((2R,3S,5R)-3-Acetoxy-5-(5-bromo-4-chloro-2-oxopyrimidin-1(2H)-yl)tetrahydrofuran-2-yl)methyl acetate (**5**).* A solution of 5-bromo-3′,5′-diacetyl-2′-deoxyuridine (0.80 g, 2.05 mmol) and PPh_3 (1.34 g, 5.13 mmol), in a mixture of CH_2Cl_2 and CCl_4 (10 + 10 mL), was refluxed for 40 min. The solvent was removed in vacuo and the residue was purified by silica gel flash-column chromatography, using a gradient elution (EtOAc/CH_2Cl_2; 5:95 to 15:85), to yield compound **5** as a white solid (0.63 g, 75% yield). ^{1}H NMR (400 MHz, $CDCl_3$) δ 8.20 (s, 1H), 6.04 (t, J = 6.4 Hz, 1H), 5.12 (dt, J = 6.3, 2.9 Hz, 1H), 4.38−4.20 (m, 3H), 2.73 (ddd, J = 14.5, 6.0, 3.0 Hz, 1H), 2.14 (dt, J = 14.3, 6.7 Hz, 1H), 2.03 (s, 3H), 2.00 (s, 3H).^{13}C{^{1}H} NMR (101 MHz, $CDCl_3$) δ 170.2, 170.0, 165.5, 151.4, 144.0, 100.0, 97.1, 88.1, 83.5, 77.6, 77.3, 76.9, 73.4, 63.2, 60.3, 53.6, 38.9, 21.0, 20.8, 14.1. HRMS (ESI-TOF) m/z: [M + Na]$^+$ calcd for $C_{13}H_{14}BrClN_2O_5Na^+$ 430.9616; found 430.9628.

*5-Bromo-3′,5′-diacetyl-N-4-(2-hydroxytetraethylisoindolinyl)-2′-deoxycytidine (**7**).* To a solution of compound **4** (262 mg, 0.706 mmol) and compound **5** (346 mg, 0.847 mmol) in $CHCl_3$ (10 mL) was added Et_3N (180 μL, 1.29 mmol), and the solution was stirred at 22 °C for 16 h. The solvent was removed in vacuo, and the crude product was used in the next reaction without purification. ^{1}H NMR (400 MHz, $CDCl_3$) δ 7.97 (s, 1H), 7.84 (s, 1H), 7.39 (s, 1H), 6.80 (s, 1H), 6.31−6.20 (m, 1H), 5.21 (dt, J = 5.9, 2.5 Hz, 1H), 4.38 (d, J = 3.3 Hz, 2H), 4.32 (d, J = 3.0 Hz, 1H), 2.71 (ddd, J = 14.2, 5.6, 2.4 Hz, 1H), 2.15 (s, 3H), 2.10 (s, 3H), 1.85−1.67 (m, 8H), 0.87 (q, J = 7.4 Hz, 13H). ^{13}C{^{1}H} NMR (101 MHz, $CDCl_3$) δ 170.4, 170.2, 157.0, 153.4, 148.7, 140.4, 125.5, 116.1, 88.6, 86.9, 82.9, 77.2, 73.9, 63.7, 50.8, 39.0, 32.9, 32.7, 31.9, 29.7, 29.4, 22.7, 20.9, 20.9, 14.1, 8.8, 8.7 ppm. HRMS (ESI-TOF) m/z: [M + H]$^+$ calcd for $C_{29}H_{40}BrN_4O_7^+$: 635.2075; found 635.2063.

*7,7,9,9-Tetraethyl-3-((2R,4S,5R)-4-hydroxy-5-(hydroxymethyl)-tetrahydrofuran-2-yl)-7,8,9,11-tetrahydropyrimido[4′,5′:5,6][1,4]-oxazino[2,3-f]isoindol-2(3H)-one (**EÇf**).* To a solution of compound **7** (449 mg, 0.706 mmol) in abs. EtOH (50 mL) was added KF (1.0 g, 17.0 mmol), and the mixture was refluxed for 42 h. The reaction mixture was cooled to room temperature, and the salts were filtered from the solution. The filtrate was concentrated in vacuo, and the residue was purified by flash-column chromatography, using a gradient elution (100:0 to 75:25, CH_2Cl_2/MeOH), to yield **EÇf** (187 mg, 56%) as a pale yellow solid. ^{1}H NMR (400 MHz, CD_3OD) δ 7.67 (s, 1H), 6.67 (s, 1H), 6.44 (s, 1H), 6.21 (t, J = 6.5 Hz, 1H), 4.37 (dt, J = 6.6, 3.7 Hz, 1H), 3.91 (q, J = 3.0 Hz, 1H), 3.86−3.65 (m, 2H), 2.31 (ddd, J = 13.3, 5.8, 3.6 Hz, 1H), 2.13 (dt, J = 13.4, 6.6 Hz, 1H), 1.61 (qd, J = 14.0, 11.6, 7.3 Hz, 8H), 0.81 (dd, J = 8.8, 4.8 Hz, 12H) ppm. ^{13}C{^{1}H} NMR (101 MHz, CD_3OD) δ 156.4, 155.9,

https://dx.doi.org/10.1021/acs.joc.9b02988
J. Org. Chem. 2020, 85, 4036−4046

144.2, 143.5, 143.3, 129.9, 127.0, 123.5, 112.0, 110.8, 89.1, 87.6, 72.2, 70.2, 70.1, 62.8, 42.0, 34.4, 34.3, 9.4, 9.3 ppm. HRMS (ESI-TOF) m/z: $[M + H]^+$ calcd for $C_{25}H_{35}N_4O_5^+$: 471.2602; found 471.2603.

*3-((2R,4S,5R)-4-((tert-Butyldimethylsilyl)oxy)-5-(((tert-butyldimethylsilyl)oxy)methyl)tetrahydrofuran-2-yl)-7,7,9,9-tetraethyl-7,8,9,11-tetrahydropyrimido[4′,5′:5,6][1,4]oxazino[2,3-f]isoindol-2(3H)-one (**TBDMS-EÇf**).* A solution of **EÇf** (2.30 g, 4.89 mmol), TBDMSCl (2.21 g, 14.7 mmol), and imidazole (0.992 g, 14.7 mmol) in a mixture of pyridine and dimethylformamide (DMF) (1:1, 20 mL) was stirred at 22 °C for 24 h. The reaction mixture was poured onto ice and extracted with EtOAc (3 × 100 mL); the combined organic phases were dried over Na_2SO_4, and the solvent removed was in vacuo. The residue was purified by flash-column chromatography, using a gradient elution (100:0 to 90:10, CH_2Cl_2/MeOH), to yield **TBDMS-EÇf** (3.38 g, 99%) as a pale yellow solid. ^{1}H NMR (400 MHz, $CDCl_3$) δ 7.45 (s, 2H), 6.33 (s, 1H), 6.25 (t, J = 6.1 Hz, 1H), 4.42−4.35 (m, 1H), 3.96−3.83 (m, 2H), 3.83−3.71 (m, 1H), 2.33 (ddd, J = 13.2, 6.2, 4.3 Hz, 1H), 2.08−1.95 (m, 2H), 1.67 (s, 8H), 0.96 (s, 9H), 0.89 (s, 21H), 0.15 (d, J = 8.4 Hz, 6H), 0.09−0.04 (m, 9H) ppm. ^{13}C{^{1}H} NMR (101 MHz, $CDCl_3$) δ 154.7, 153.8, 128.1, 108.9, 87.7, 85.9, 77.4, 71.4, 62.7, 41.9, 33.7, 29.8, 26.2, 26.0, 25.9, 22.8, 18.6, 18.1, 8.9, 1.2, −4.5, −4.7, −5.3, −5.3 ppm. HRMS (ESI-TOF) m/z: $[M + H]^+$ calcd for $C_{37}H_{63}N_4O_5Si_2^+$: 699.4332; found 699.4280.

*3-((2R,4S,5R)-4-((tert-Butyldimethylsilyl)oxy)-5-(((tert-butyldimethylsilyl)oxy)methyl)tetrahydrofuran-2-yl)-7,7,9,9-tetraethyl-8-oxyl-7,8,9,11-tetrahydropyrimido[4′,5′:5,6][1,4]oxazino-[2,3-f]isoindol-2(3H)-one (**9**).* To a solution of **TBDMS-EÇf** (400 mg, 0.572 mmol) in CH_2Cl_2 (10 mL) was added NaN_3 (198 mg, 1.14 mmol), and the solution was stirred for 15 min at 22 °C. *m*-CPBA (74.9 mg, 1.14 mmol) was added and the solution was stirred for 4 h. The reaction mixture was concentrated in vacuo, and the crude product was purified by flash-column chromatography, using a gradient elution (100:0 to 83:17, CH_2Cl_2/MeOH), to yield **9** (339 mg, 83%) as a bright yellow solid. HRMS (ESI-TOF) m/z: $[M + Na]^+$ calcd for $C_{37}H_{61}N_4O_6Si_2Na^{\bullet+}$: 736.4022; found 736.3997.

*7,7,9,9-Tetraethyl-8-oxidanyl-3-((2R,4S,5R)-4-hydroxy-5-(hydroxymethyl)tetrahydrofuran-2-yl)-7,8,9,11-tetrahydropyrimido[4′,5′:5,6][1,4]oxazino[2,3-f]isoindol-2(3H)-one (**EÇ**).* To a solution of **9** (500 mg, 0.700 mmol) in anhydrous tetrahydrofuran (THF) (3 mL) was added TBAF (2.03 mL, 7.00 mmol), and the solution was stirred at 22 °C for 12 h. The solvent was removed in vacuo and the residue was purified by flash-column chromatography, using a gradient elution (100:0 to 75:25, CH_2Cl_2/MeOH), to yield **EÇ** (310 mg, 91%) as a yellow solid. HRMS (ESI-TOF) m/z: $[M + Na]^+$ calcd for $C_{25}H_{33}N_4O_6Na^{\bullet+}$: 508.2298; found 508.2292

*3-((2R,4S,5R)-5-((Bis(4-methoxyphenyl)(phenyl)methoxy)-methyl)-4-hydroxytetrahydrofuran-2-yl)-7,7,9,9-tetraethyl-8-oxidanyl-7,8,9,11-tetrahydropyrimido[4′,5′:5,6][1,4]oxazino[2,3-f]-isoindol-2(3H)-one (**DMT-EÇ**).* Residual MeOH was co-evaporated with toluene (3 × 5 mL) from **EÇ** (477 mg, 0.982 mmol), followed by sequential addition of pyridine (10 mL), DMTrCl (433 mg, 1.28 mmol), and 4-(dimethylamino)pyridine (DMAP) (27.0 mg, 0.197 mmol). The solution was stirred at 22 °C for 6 h, MeOH (400 μL) was added, and the solvent was removed in vacuo. The residue was purified by flash-column chromatography, using a gradient elution (1:99:0 to 1:95.5:3.5, Et_3N/CH_2Cl_2/MeOH), to yield **DMT- EÇ** (735 mg, 95%) as a yellow solid. HRMS (ESI-TOF) m/z: $[M + Na]^+$ calcd for $C_{46}H_{51}N_4O_8Na^{\bullet+}$: 810.3601; found 810.3599

*(2R,3S,5R)-2-((Bis(4-methoxyphenyl)(phenyl)methoxy)methyl)-5-(7,7,9,9-tetraethyl-8-oxidanyl-2-oxo-7,8,9,11-tetrahydropyrimido-[4′,5′:5,6][1,4]oxazino[2,3-f]isoindol-3(2H)-yl)tetrahydrofuran-3-yl (2-cyanoethyl) diisopropylphosphoramidite (**11**).* To a solution of **DMT-EÇ** (100 mg, 0.127 mmol) in CH_2Cl_2 (5 mL) were added diisopropylammonium tetrazolide (171 mg, 1.52 mmol) and 2-cyanoethyl *N*,*N*,*N*′,*N*′-tetraisopropylphosphorodiamidite (52 μL, 0.17 mmol). The resulting solution was stirred at 22 °C for 2 h. CH_2Cl_2 (50 mL) was added, and the organic phase was washed sequentially with satd. aq. $NaHCO_3$ (3 × 50 mL) and brine (50 mL), was dried over Na_2SO_4, and was concentrated in vacuo. The residue was dissolved in a minimum amount of CH_2Cl_2 (few drops) and was followed by a slow addition of *n*-hexane (40−50 mL) at 22 °C. The solvent was decanted from the precipitate and was discarded. This procedure was repeated four times to give **11** (100 mg, 80%) as a yellowish solid. ^{31}P NMR (162 MHz, $CDCl_3$): δ 150.27, 149.35 ppm. HRMS (ESI-TOF) m/z: $[M + Na]^+$ calcd for $C_{55}H_{68}N_6O_9Na^{\bullet+}$: 1010.4678; found 1010.4578,

*5-Bromo-3′,5′-diacetyl-N-4-(2-hydroxytetraethylisoindolinyl)-2′-methoxycytidine (**8**).* To a solution of compound **4** (592 mg, 2.03 mmol) and **6** (1021 mg, 2.32 mmol) in $CHCl_3$ (10 mL) was added Et_3N (180 μL, 1.29 mmol), and the solution was stirred at 22 °C for 16 h. The solvent was removed in vacuo, and the crude product was used in the next reaction without purification. ^{1}H NMR (400 MHz, $CDCl_3$) δ 8.30 (s, 1H), 7.98 (s, 1H), 7.82 (s, 1H), 7.57 (s, 1H), 6.91 (s, 1H), 5.90−5.79 (m, 1H), 4.73 (dd, J = 9.3, 5.0 Hz, 1H), 4.47−4.29 (m, 3H), 4.05−3.97 (m, 1H), 3.51 (s, 1H), 2.17 (s, 3H), 2.14 (s, 3H), 1.80−1.50 (m, 8H), 0.84 (dtd, J = 10.3, 7.4, 3.8 Hz, 12H).^{13}C{^{1}H} NMR (101 MHz, $CDCl_3$) δ 170.2, 170.1, 170.04, 169.97, 166.0, 157.6, 153.5, 153.1, 146.1, 145.6, 143.9, 142.5, 140.3, 127.5, 119.1, 116.3, 100.0, 89.8, 89.5, 88.4, 87.5, 81.7, 81.7, 78.8, 78.4, 77.5, 77.4, 77.2, 76.9, 68.9, 68.7, 68.6, 68.4, 61.4, 61.1, 59.0, 58.9, 53.5, 33.7, 33.5, 29.6, 21.09, 21.07, 20.51, 20.49, 8.9. HRMS (ESI-TOF) m/z: $[M + H]^+$ calcd for $C_{30}H_{42}BrN_4O_8^+$: 665.2181; found 665.2165.

*7,7,9,9-Tetraethyl-3-((2R,3R,4R,5R)-4-hydroxy-5-(hydroxymethyl)-3-methoxytetrahydrofuran-2-yl)-7,8,9,11-tetrahydropyrimido-[4′,5′:5,6][1,4]oxazino[2,3-f]isoindol-2(3H)-one (**EÇmf**).* To a solution of compound **8** (1.35 g, 2.03 mmol) in abs. EtOH (200 mL) was added KF (1.18 g, 20.2 mmol), and the mixture was refluxed for 42 h. The mixture was cooled to room temperature, and the salts were removed by filtration. The filtrate was concentrated in vacuo, and the residue was purified by flash-column chromatography, using a gradient elution (100:0 to 75:25, CH_2Cl_2/MeOH), to yield **EÇmf** (567 mg, 60%) as a pale yellow solid. ^{1}H NMR (400 MHz, CD_3OD) δ 7.91 (s, 1H), 6.82−6.74 (m, 1H), 6.72 (s, 1H), 5.88 (d, J = 2.6 Hz, 1H), 4.23 (dd, J = 7.1, 5.1 Hz, 1H), 4.02−3.87 (m, 2H), 3.85−3.73 (m, 2H), 3.57 (s, 3H), 2.02−1.96 (m, 8H), 1.00 (td, J = 7.3, 4.7 Hz, 12H) ppm. ^{13}C{^{1}H} NMR (101 MHz, CD_3OD) δ 156.1, 155.7, 144.9, 138.7, 138.0, 129.6, 129.3, 123.9, 112.4, 111.6, 89.7, 85.6, 85.5, 75.4, 69.4, 61.2, 59.0, 49.7, 49.6, 49.5, 49.4, 49.3, 49.2, 49.1, 48.9, 48.7, 48.5, 48.0, 31.9, 9.3, 8.78, 8.77 ppm. HRMS (ESI-TOF) m/z: $[M + H]^+$ calcd for $C_{26}H_{37}N_4O_6^+$: 501.2708; found 501.2706.

*3-((2R,3R,4R,5R)-4-((tert-Butyldimethylsilyl)oxy)-5-(((tert-butyldimethylsilyl)oxy)methyl)-3-methoxytetrahydrofuran-2-yl)-7,7,9,9-tetraethyl-7,8,9,11-tetrahydropyrimido[4′,5′:5,6][1,4]-oxazino[2,3-f]isoindol-2(3H)-one (**TBDMS-EÇmf**).* A solution of **EÇmf** (416 mg, 0.832 mmol), TBDMSCl (376 mg, 2.50 mmol), and imidazole (170 mg, 2.50 mmol) in a mixture of pyridine and DMF (1:1, 10 mL) was stirred at 22 °C for 24 h. The reaction mixture was poured onto ice and extracted with EtOAc (3 × 100 mL), the combined organic phases were dried over Na_2SO_4, and the solvent was removed in vacuo. The residue was purified by flash-column chromatography, using a gradient elution (100:0 to 90:10, CH_2Cl_2/MeOH), to yield **TBDMS-EÇmf** (600 mg, 99%) as a pale yellow solid. HRMS (ESI-TOF) m/z: $[M + H]^+$ calcd for $C_{38}H_{65}N_4O_6Si_2^+$: 729.4437 $[M + H]^+$; found 729.4436.

*3-((2R,3R,4R,5R)-4-((tert-Butyldimethylsilyl)oxy)-5-(((tert-butyldimethylsilyl)oxy)methyl)-3-methoxytetrahydrofuran-2-yl)-7,7,9,9-tetraethyl-8-oxyl-7,8,9,11-tetrahydropyrimido[4′,5′:5,6]-[1,4]oxazino[2,3-f]isoindol-2(3H)-one (**10**).* To a solution of **TBDMS-EÇmf** (153 mg, 0.249 mmol) in CH_2Cl_2 (10 mL) was added NaN_3 (65 mg, 1.0 mmol), and the solution was stirred at 22 °C for 15 min. *m*-CPBA (86 mg, 0.5 mmol) was added, the solution was stirred for 30 h, the solvent was removed in vacuo, and the crude product was purified by flash-column chromatography, using a gradient elution (100:0 to 83:17, CH_2Cl_2/MeOH), to yield **10** (150 mg, 81%) as a bright yellow solid. HRMS (ESI-TOF) m/z: $[M + Na]^+$ calcd for $C_{38}H_{63}N_4O_7Si_2Na^{\bullet+}$: 766.4127; found 766.4069.

7,7,9,9-Tetraethyl-8-oxyl-3-((2R,3R,4R,5R)-4-hydroxy-5-(hydroxymethyl)-3-methoxytetrahydrofuran-2-yl)-7,8,9,11-tetrahydropyrimido[4′,5′:5,6][1,4]oxazino[2,3-f]isoindol-2(3H)-one

https://dx.doi.org/10.1021/acs.joc.9b02988
J. Org. Chem. 2020, 85, 4036−4046

*(**EÇm**).* To a solution of **EÇm** (377 mg, 0.507 mmol) in THF (3 mL) was added TBAF (1.50 ml, 5.07 mmol), and the reaction mixture was stirred at 22 °C for 12 h. The solvent was removed in vacuo, and the residue was purified by flash-column chromatography, using a gradient elution (100:0 to 90:10, CH_2Cl_2/MeOH), to yield **EÇm** (249 mg, 94%) as a yellow solid. HRMS (ESI-TOF) *m*/*z*: $[M + Na]^+$ calcd for $C_{26}H_{35}N_4O_7Na^{\bullet+}$: 538.2403; found 538.2399.

*3-((2R,3R,4R,5R)-5-((Bis(4-methoxyphenyl)(phenyl)methoxy)-methyl)-4-hydroxy-3-methoxytetrahydrofuran-2-yl)-7,7,9,9-tetraethyl-8-oxidanyl-7,8,9,11-tetrahydropyrimido[4′,5′:5,6][1,4]-oxazino[2,3-f]isoindol-2(3H)-one (**EÇm-DMT**).* Residual MeOH was co-evaporated with toluene (3 × 5 mL) from **EÇm** (400 mg, 0.776 mmol), followed by sequential addition of pyridine (4 mL), DMTCl (315 mg, 0.930 mmol), and DMAP (18.6 mg, 0.155 mmol). The solution was stirred at 22 °C for 14 h, MeOH (400 μL) was added, and the solvent was removed in vacuo. The residue was purified by flash-column chromatography, using a gradient elution (99:1:0 to 98:1:1, CH_2Cl_2/Et_3N/MeOH), to yield **EÇm-DMT** (514 mg, 81%) as a yellow solid. HRMS (ESI-TOF) *m*/*z*: $[M + Na]^+$ calcd for $C_{47}H_{53}N_4O_9Na^{\bullet+}$: 840.3705; found 840.3646.

*(2R,3R,4R,5R)-2-((Bis(4-methoxyphenyl)(phenyl)methoxy)-methyl)-4-methoxy-5-(7,7,9,9-tetraethyl-8-oxidanyl-2-oxo-7,8,9,11-tetrahydropyrimido[4′,5′:5,6][1,4]oxazino[2,3-f]isoindol-3(2H)-yl)tetrahydrofuran-3-yl (2-cyanoethyl) diisopropylphosphoramidite (**12**).* A solution of **EÇm-DMT** (225 mg, 0.275 mmol) in CH_2Cl_2 (1 mL) was treated with diisopropylammonium tetrazolide (70.6 mg, 0.413 mmol) and 2-cyanoethyl *N*,*N*,*N*′,*N*′-tetraisopropylphosphorodiamidite (262 μL, 0.825 mmol). The solution was stirred at 22 °C for 18 h. CH_2Cl_2 (25 mL) was added, and the organic phase was washed sequentially with satd. aq. $NaHCO_3$ (3 × 30 mL) and brine (50 mL), was dried with Na_2SO_4, and was concentrated in vacuo. The residue was dissolved in a minimum amount of CH_2Cl_2 (few drops), followed by a slow addition of *n*-hexane (40−50 mL) at 22 °C. The solvent was decanted from the precipitate and was discarded. This procedure was repeated six times to yield **12** (199 mg, 71%) as a yellow solid. ^{31}P NMR (162 MHz, $CDCl_3$): δ 151.03, 150.16 ppm.

*3-((2R,3R,4R,5R)-4-((tert-Butyldimethylsilyl)oxy)-5-(((tert-butyldimethylsilyl)oxy)methyl)-3-methoxytetrahydrofuran-2-yl)-7,7,9,9-tetraethyl-2-oxo-2,7,9,11-tetrahydropyrimido[4′,5′:5,6]-[1,4]oxazino[2,3-f]isoindol-8(3H)-yl benzoate (**13**).* To a solution of **10** (227 mg, 0.305 mmol) in 1,4-dioxane (30 mL) was added L-ascorbic acid (537 mg, 3.05 mmol) in H_2O (5 mL). The solution was stirred at 60 °C for 24 h, after which CH_2Cl_2 (30 mL) and H_2O (30 mL) were added, and the mixture was stirred vigorously for 2 min. The organic phase was filtered through a short column of Na_2SO_4 into a solution of BzCl (198 μL, 1.53 mmol) and Et_3N (220 μL, 1.53 mmol) in CH_2Cl_2 (10 mL). The solution was stirred at 22 °C for 2 h, was washed with satd. aq. $NaHCO_3$ (3 × 100 mL), and the organic phase was dried over Na_2SO_4 and concentrated in vacuo. The residue was purified by flash-column chromatography, using a gradient elution (100:0 to 90:10, CH_2Cl_2/MeOH), to yield **13** (259 mg, quant.) as a yellow solid. ^1H NMR (400 MHz, $CDCl_3$) δ 8.18−8.12 (m, 1H), 8.12−8.05 (m, 2H), 7.84 (s, 1H), 7.62−7.53 (m, 2H), 7.53−7.42 (m, 3H), 6.39 (s, 1H), 5.88 (d, *J* = 9.6 Hz, 1H), 4.29−4.20 (m, 1H), 4.13 (dd, *J* = 12.1, 2.0 Hz, 1H), 4.05 (d, *J* = 8.9 Hz, 1H), 3.82 (dd, *J* = 11.9, 1.6 Hz, 1H), 3.65 (s, 4H), 2.23−1.56 (m, 8H), 0.96 (d, *J* = 39.9 Hz, 30H), 0.21 (d, *J* = 7.0 Hz, 6H), 0.10 (d, *J* = 5.2 Hz, 6H) ppm. $^{13}C\{^1H\}$ NMR (101 MHz, $CDCl_3$) δ 165.9, 155.3, 153.4, 142.0, 137.7, 137.4, 133.3, 133.0, 130.2, 129.6, 128.5, 128.3, 127.6, 125.6, 122.0, 113.3, 110.1, 87.9, 84.1, 83.1, 74.4, 74.2, 68.0, 60.5, 57.9, 30.2, 29.2, 26.3, 25.8, 18.7, 18.1, 9.5, 8.7, −4.5, −4.9, −5.2, −5.4 ppm. HRMS (ESI-TOF) *m*/*z*: $[M + Na]^+$ calcd for $C_{45}H_{68}N_4O_8Si_2Na^+$: 871.4473; found 871.4468

*7,7,9,9-Tetraethyl-3-((2R,3R,4R,5R)-4-hydroxy-5-(hydroxymethyl)-3-methoxytetrahydrofuran-2-yl)-2-oxo-2,7,9,11-tetrahydropyrimido[4′,5′:5,6][1,4]oxazino[2,3-f]isoindol-8(3H)-yl benzoate (**Bz-EÇm**).* To a solution of compound **13** (250 mg, 0.294 mmol) in THF (10 mL) was added TBAF (0.863 mL, 2.95 mmol, 1.0 M in THF), and the reaction was stirred at 22 °C for 12 h. The solvent was removed in vacuo, and the residue was purified by flash-column chromatography, using a gradient elution (100:0 to 90:10, CH_2Cl_2/MeOH), to yield **Bz-EÇm** (168 mg, 92%) as a yellow solid. ^1H NMR (400 MHz, $CDCl_3$) δ 8.33−8.25 (m, 3H), 7.91−7.84 (m, 1H), 7.75 (t, *J* = 7.7 Hz, 2H), 6.83 (d, *J* = 19.3 Hz, 2H), 6.18 (d, *J* = 2.3 Hz, 1H), 4.51 (dd, *J* = 7.2, 5.0 Hz, 1H), 4.34−4.18 (m, 2H), 4.07 (dd, *J* = 12.3, 2.3 Hz, 2H), 3.86 (s, 3H), 2.42−1.82 (m, 9H), 1.31−1.00 (m, 14H) ppm. $^{13}C\{^1H\}$ NMR (101 MHz, $CDCl_3$) δ 166.1, 153.2, 141.9, 138.6, 137.0, 133.0, 129.1, 128.8, 128.3, 128.1, 124.2, 123.0, 111.6, 110.8, 88.1, 84.1, 83.8, 77.4, 74.0, 73.9, 67.5, 59.5, 57.8, 48.7, 48.5, 48.3, 48.1, 47.9, 47.7, 47.5, 29.9, 29.2, 28.7, 8.7, 7.9 ppm. HRMS (ESI-TOF) *m*/*z*: $[M + Na]^+$ calcd for $C_{33}H_{40}N_4O_8Na^+$: 643.2738; found 643.2746

*3-((2R,3R,4R,5R)-5-((Bis(4-methoxyphenyl)(phenyl)methoxy)-methyl)-4-hydroxy-3-methoxytetrahydrofuran-2-yl)-7,7,9,9-tetraethyl-2-oxo-2,7,9,11-tetrahydropyrimido[4′,5′:5,6][1,4]oxazino-[2,3-f]isoindol-8(3H)-yl benzoate (**Bz-EÇm-DMT**).* Residual MeOH was co-evaporated with toluene (3 × 5 mL) from **Bz-EÇm** (118 mg, 0.192 mmol), followed by sequential addition of pyridine (4 mL), DMTCl (192 mg, 0.572 mmol), and DMAP (12.0 mg, 0.0952 mmol). The solution was stirred at 22 °C for 14 h, MeOH (400 μL) was added, and the solvent was removed in vacuo. The residue was purified by flash-column chromatography, using a gradient elution (99:1:0 to 98:1:1, CH_2Cl_2/Et_3N/MeOH), to yield **Bz-EÇm-DMT** (151 mg, 86%) as a yellow solid. ^1H NMR (400 MHz, $CDCl_3$) δ 8.02−7.96 (m, 2H), 7.57−7.46 (m, 2H), 7.46−7.35 (m, 5H), 7.35−7.27 (m, 5H), 7.27−7.16 (m, 3H), 7.10 (t, *J* = 7.3 Hz, 2H), 6.82−6.73 (m, 5H), 6.08 (d, *J* = 18.3 Hz, 1H), 5.82 (s, 1H), 4.35 (s, 1H), 4.01−3.88 (m, 1H), 3.76 (d, *J* = 5.3 Hz, 1H), 3.67 (s, 7H), 3.62 (s, 3H), 3.45 (s, 3H), 1.98−1.58 (m, 9H), 0.95−0.78 (m, 13H) ppm. $^{13}C\{^1H\}$ NMR (101 MHz, $CDCl_3$) δ 166.0, 158.6, 158.5, 155.2, 153.8, 145.1, 141.7, 137.2, 135.3, 133.0, 130.4, 130.1, 129.6, 129.5, 128.5, 127.95, 127.92, 126.7, 125.3, 121.4, 113.3, 113.2, 110.3, 87.8, 86.7, 83.8, 82.7, 74.3, 74.2, 68.5, 58.4, 55.2, 46.0, 30.2, 29.7, 29.2, 9.4, 9.1, 8.7 ppm. HRMS (ESI-TOF) *m*/*z*: $[M + Na]^+$ calcd for $C_{54}H_{58}N_4O_{10}Na^+$: 945.4045; found 945.4012

*3-((2R,3R,4R,5R)-5-((Bis(4-methoxyphenyl)(phenyl)methoxy)-methyl)-4-(((2-cyanoethoxy)(diisopropylamino)phosphaneyl)oxy)-3-methoxytetrahydrofuran-2-yl)-7,7,9,9-tetraethyl-2-oxo-2,7,9,11-tetrahydropyrimido[4′,5′:5,6][1,4]oxazino[2,3-f]isoindol-8(3H)-yl benzoate (**14**).* A solution of **Bz-EÇm-DMT** (150 mg, 0.163 mmol) in CH_2Cl_2 (3 mL) was treated with diisopropylammonium tetrazolide (41.8 mg, 0.244 mmol) and 2-cyanoethyl *N*,*N*,*N*′,*N*′-tetraisopropylphosphorodiamidite (155 μL, 0.488 mmol). The solution was stirred at 22 °C for 18 h. CH_2Cl_2 (25 mL) was added, and the organic phase was washed sequentially with satd. aq. $NaHCO_3$ (3 × 30 mL) and brine (50 mL), was dried over Na_2SO_4, and was concentrated in vacuo. The residue was dissolved in a minimum amount of CH_2Cl_2 (few drops), followed by a slow addition of *n*-hexane (40−50 mL) at 22 °C. The solvent was decanted from the precipitate and discarded. This procedure was repeated six times to yield **14** (130 mg, 71%) as a yellow solid. ^1H NMR (400 MHz, $CDCl_3$) δ 8.12−8.03 (m, 4H), 7.68 (d, *J* = 19.9 Hz, 2H), 7.62−7.54 (m, 3H), 7.54−7.44 (m, 9H), 7.44−7.34 (m, 9H), 7.30 (td, *J* = 7.8, 2.4 Hz, 5H), 7.20 (t, *J* = 7.3 Hz, 2H), 6.86 (dtd, *J* = 8.8, 6.7, 6.2, 3.4 Hz, 8H), 6.23−5.87 (m, 4H), 4.57 (d, *J* = 15.0 Hz, 1H), 4.34 (d, *J* = 12.8 Hz, 1H), 4.24 (d, *J* = 7.8 Hz, 2H), 3.90 (ddd, *J* = 19.9, 10.0, 5.4 Hz, 3H), 3.81 (d, *J* = 2.2 Hz, 1H), 3.77 (d, *J* = 2.3 Hz, 12H), 3.63 (d, *J* = 2.6 Hz, 8H), 3.61−3.53 (m, 5H), 3.52−3.41 (m, 4H), 2.63 (t, *J* = 6.1 Hz, 2H), 2.42 (t, *J* = 6.4 Hz, 2H), 2.16−1.50 (m, 23H), 1.17 (dd, *J* = 15.1, 6.8 Hz, 19H), 1.04 (d, *J* = 6.7 Hz, 7H) ppm. $^{13}C\{^1H\}$ NMR (101 MHz, $CDCl_3$) δ 158.7, 158.6, 133.0, 130.5, 130.3, 129.6, 128.5, 128.1, 127.9, 113.2, 110.3, 77.2, 74.3, 74.2, 58.0, 55.3, 55.2, 43.4, 43.2, 31.6, 24.7, 24.7, 24.6, 24.5, 22.7, 20.3, 14.1, 9.4, 8.7 ppm. ^{31}P NMR (162 MHz, $CDCl_3$) δ 150.84, 150.02. HRMS (ESI-TOF) *m*/*z*: $[M + Na]^+$ calcd for $C_{63}H_{75}N_6O_{11}PNa^+$: 1145.5129; found 1145.5098.

DNA and RNA Syntheses and Purification. Unmodified phosphoramidites (2′-deoxy for DNA and 2′O-TBDMS protected for RNA) were dissolved in CH_3CN (0.1 M), and phosphoramidites **11**, **12**, and **14** were dissolved in 1,2-dichloroethane (0.1 M). 5-Ethylthiotetrazole (0.25 M in CH_3CN) was used as a coupling agent

https://dx.doi.org/10.1021/acs.joc.9b02988
J. Org. Chem. 2020, 85, 4036−4046

for DNA and 5-benzylthiotetrazole (0.25 M in CH_3CN) for RNA. The coupling time was set to 1.5 min for unmodified phosphoramidites of DNA, 5 min for the **EÇ**-modified phosphoramidite, **11** and 7 min for both unmodified phosphoramidites of RNA and **EÇm**-modified phosphoramidites **12** and **14**. After completion of the DNA synthesis, the DNAs were cleaved from the resin and deprotected in a sat. aq. NH_3 solution at 55 °C for 8 h, after which the solvent was removed in vacuo. After completion of RNA synthesis, the RNAs synthesized using phosphoramidite **12** were deprotected and cleaved from the resin in a 1:1 solution (2 mL) of CH_3NH_2 (8 M in EtOH) and NH_3 (33% w/w in H_2O) at 65 °C for 1 h, while the oligonucleotides synthesized using phosphoramidite **14** were deprotected and cleaved from the resin in a 1:1 solution (2 mL) of CH_3NH_2 (40% in H_2O) and NH_3 (40% w/w in H_2O) at 65 °C for 2.5 h. The solvent was removed in vacuo, and the 2′O-TBDMS groups were removed by incubation in a solution of $Et_3N{\cdot}3HF$ (300 μL) in DMF (100 μL) at 55 °C for 1.5 h, followed by addition of deionized and sterilized water (100 μL). This solution was transferred to a 50 mL Falcon tube, *n*-butanol (20 mL) was added, the mixture was stored at −20 °C for 14 h, was centrifuged at 4 °C, and the solvent was decanted from the RNA pellet.

All oligonucleotides were subsequently purified by 20% DPAGE and were extracted from the gel slices using the "crush and soak method" with Tris buffer (250 mM NaCl, 10 mM Tris, 1 mM Na_2EDTA, pH 7.5). The solutions were filtered through GD/X syringe filters (0.45 μm, 25 mm diameter, Whatman) and were subsequently desalted using Sep-Pak cartridges (Waters), following the instructions provided by the manufacturer. Dried oligonucleotides were dissolved in deionized and sterilized water (200 μL for each oligonucleotide).

Enzymatic Digestion of DNA and RNA and HPLC Analysis. To the oligonucleotide (4 nmol) in sterile water (8 μL) were added calf intestinal alkaline phosphatase (1 μL, 2 U), snake venom phosphodiesterase I (4 μL, 0.2 U), nuclease P1 from Penicillium citrinum (5 μL, 1.5 U), and Tris buffer (2 μL, 0.5 M Tris and 0.1 M $MgCl_2$). The samples were incubated at 37 °C for 50 h, after which they were analyzed by HPLC chromatography (Figures S30 and S31).

CD Measurements. To determine if **EÇ** and **EÇm** labels had any effect on the DNA and RNA duplex conformation, circular dichroism (CD) spectra of all unmodified duplexes and their spin-labeled counterparts were recorded. DNA and RNA duplexes were prepared by dissolving complementary single-stranded oligonucleotides (2.5 nmol) of each in a phosphate buffer (100 μL; 10 mM phosphate, 100 mM NaCl, 0.1 mM Na_2EDTA, pH 7.0) and annealed. The annealed samples were diluted to 200 μL with the same buffer (Figure S32).

Thermal Denaturing Experiments. To determine if **EÇ** or **EÇm** affected the stability of the DNA or RNA duplexes, the thermal denaturation curves of unmodified and spin-labeled oligomers were determined. Both DNA and RNA samples were prepared by dissolving 4.0 nmol of each strand in a phosphate buffer (100 μL; 10 mM phosphate, 100 mM NaCl, 0.1 mM Na_2EDTA, pH 7.0), were annealed, were diluted to 1.0 mL with the phosphate buffer (pH 7.0), and were degassed with Ar. The samples were heated up from 22 to 90 °C (1.0 °C/min), and the absorbance at 260 nm was recorded at 1.0 °C intervals (Table 1 and Figure S33).

CW−EPR Measurements and Spin Counting. Samples of spin-labeled oligonucleotides for EPR measurements were prepared by dissolving spin-labeled, single-stranded DNA or RNA (2.0 nmol) in phosphate buffer (10 μL, 10 mM phosphate, 100 mM NaCl, 0.1 mM Na_2EDTA, pH 7.0, oligonucleotide final conc. 200 μM) (Figure S34). The amount of spin labels in each oligonucleotide was determined by spin counting. A stock solution of 4-hydroxy-TEMPO (1.0 M) was prepared in phosphate buffer (10 mM phosphate, 100 mM NaCl, 0.1 mM Na_2EDTA, pH 7.0). The stock solution was diluted into samples of different concentrations (0−0.5 mM), and each sample was measured by EPR spectroscopy. The area under the peaks of each spectrum, obtained by double integration, was plotted against its concentration to yield a standard curve and was used to determine the spin labeling efficiency with an error margin of 5−10% (Table S1).

■ ASSOCIATED CONTENT

Supporting Information

The Supporting Information is available free of charge at https://pubs.acs.org/doi/10.1021/acs.joc.9b02988.

Spin-labeled oligonucleotides and their analysis by MS and EPR spectroscopy, ^1H, ^{13}C, and ^{31}P NMR spectra, stability of **EÇ** and **EÇm** in ascorbic acid, HPLC analyses of enzymatic digestions, CD spectra of oligonucleotide duplexes, thermal denaturing experiments of spin-labeled oligonucleotides, and CW−EPR spectra of spin-labeled oligonucleotides (PDF)

■ AUTHOR INFORMATION

Corresponding Author

Snorri Th. Sigurdsson − *Department of Chemistry, Science Institute, University of Iceland 107 Reykjavik, Iceland;* orcid.org/0000-0003-2492-1456; Email: snorrisi@hi.is

Author

Haraldur Y. Juliusson − *Department of Chemistry, Science Institute, University of Iceland 107 Reykjavik, Iceland*

Complete contact information is available at: https://pubs.acs.org/10.1021/acs.joc.9b02988

Notes

The authors declare no competing financial interest.

■ ACKNOWLEDGMENTS

The authors acknowledge financial support from the Icelandic Research Fund (173727-051). The authors thank Dr. S. Jonsdottir for assistance with collecting analytical data for structural characterization of new compounds and members of the Sigurdsson research group for helpful discussions.

■ REFERENCES

(1) Blackburn, G. M.; Egli, M.; Gait, M. J.; Loakes, D.; Williams, D. M.; Flavell, A.; Allen, S.; Fisher, J. *Nucleic Acids in Chemistry and Biology*; RSC Pub., 2006.

(2) Alberts, B.; Wilson, J. H.; Johnson, A.; Hunt, T.; Lewis, J.; Roberts, K.; Raff, M.; Walter, P. *Molecular Biology of the Cell*; Garland Science, 2008.

(3) Steitz, T. A. A structural understanding of the dynamic ribosome machine. *Nat. Rev. Mol. Cell Biol.* **2008**, *9*, 242−253.

(4) Fedor, M. J.; Williamson, J. R. The catalytic diversity of RNAs. *Nat. Rev. Mol. Cell Biol.* **2005**, *6*, 399−412.

(5) Kumar, A.; Garg, S.; Garg, N. Regulation of Gene Expression. In *Reviews in Cell Biology and Molecular Medicine*; Wiley, 2014; pp 1−59.

(6) Meister, G.; Tuschl, T. Mechanisms of gene silencing by double-stranded RNA. *Nature* **2004**, *431*, 343−349.

(7) Uludag, H.; Ubeda, A.; Ansari, A. At the intersection of biomaterials and gene therapy: Progress in non-viral delivery of nucleic acids. *Front. Bioeng. Biotechnol.* **2019**, *7*, No. 131.

(8) Shi, Y. A glimpse of structural biology through X-ray crystallography. *Cell* **2014**, *159*, 995−1014.

(9) Sugiki, T.; Kobayashi, N.; Fujiwara, T. Modern technologies of solution nuclear magnetic resonance spectroscopy for three-dimensional structure determination of proteins open avenues for life scientists. *Comput. Struct. Biotechnol. J.* **2017**, *15*, 328−339.

(10) Dračínský, M.; Hodgkinson, P. Solid-state NMR studies of nucleic acid components. *RSC Adv.* **2015**, *5*, 12300−12310.

(11) Sasmal, D. K.; Pulido, L. E.; Kasal, S.; Huang, J. Single-molecule fluorescence resonance energy transfer in molecular biology. *Nanoscale* **2016**, *8*, 19928−19944.

(12) Dimura, M.; Peulen, T. O.; Hanke, C. A.; Prakash, A.; Gohlke, H.; Seidel, C. A. M. Quantitative FRET studies and integrative modeling unravel the structure and dynamics of biomolecular systems. *Curr. Opin. Chem. Biol.* **2016**, *40*, 163−185.
(13) Jeschke, G. The contribution of modern EPR to structural biology. *Emerging Top. Life Sci.* **2018**, *2*, 9−18.
(14) Gränz, M.; Erlenbach, N.; Spindler, P.; Gophane, D. B.; Stelzl, L. S.; Sigurdsson, S. T.; Prisner, T. F. Dynamics of nucleic acids at room temperature revealed by pulsed EPR spectroscopy. *Angew. Chem., Int. Ed.* **2018**, *57*, 10540−10543.
(15) Timmel, C. R.; Harmer, J. R. *Structural Information from Spin-Labels and Intrinsic Paramagnetic Centres in the Biosciences*; Springer: Berlin Heidelberg, 2014.
(16) Haugland, M. M.; Lovett, J. E.; Anderson, E. A. Advances in the synthesis of nitroxide radicals for use in biomolecule spin labelling. *Chem. Soc. Rev.* **2018**, *47*, 668−680.
(17) Giassa, I.-C.; Rynes, J.; Fessl, T.; Foldynova-Trantirkova, S.; Trantirek, L. Advances in the cellular structural biology of nucleic acids. *FEBS Lett.* **2018**, *592*, 1997−2011.
(18) Bonucci, A.; Ouari, O.; Guigliarelli, B.; Belle, V.; Mileo, E. In-cell EPR: Progress towards structural studies inside cells. *ChemBioChem* **2019**, DOI: 10.1002/cbic.201900291.
(19) Luchinat, E.; Banci, L. In-cell NMR: A topical review. *IUCrJ* **2017**, *4*, 108−118.
(20) Lippens, G.; Cahoreau, E.; Millard, P.; Charlier, C.; Lopez, J.; Hanoulle, X.; Portais, J. C. In-cell NMR: From metabolites to macromolecules. *Analyst* **2018**, *143*, 620−629.
(21) Hänsel, R.; Luh, L. M.; Corbeski, I.; Trantirek, L.; Dötsch, V. In-cell NMR and EPR spectroscopy of biomacromolecules. *Angew. Chem., Int. Ed.* **2014**, *53*, 10300−10314.
(22) Freedberg, D. I.; Selenko, P. Live cell NMR. *Annu. Rev. Biophys.* **2014**, *43*, 171−192.
(23) Narasimhan, S.; Scherpe, S.; Lucini Paioni, A.; van der Zwan, J.; Folkers, G. E.; Ovaa, H.; Baldus, M. DNP-supported solid-state NMR spectroscopy of proteins inside mammalian cells. *Angew. Chem., Int. Ed.* **2019**, *58*, 12969−12973.
(24) Padilla-Parra, S.; Tramier, M. FRET microscopy in the living cell: Different approaches, strengths and weaknesses. *BioEssays* **2012**, *34*, 369−376.
(25) Raicu, V.; Singh, D. R. FRET spectrometry: A new tool for the determination of protein quaternary structure in living cells. *Biophys. J.* **2013**, *105*, 1937−1945.
(26) Azarkh, M.; Singh, V.; Okle, O.; Seemann, I. T.; Dietrich, D. R.; Hartig, J. S.; Drescher, M. Site-directed spin-labeling of nucleotides and the use of in-cell EPR to determine long-range distances in a biologically relevant environment. *Nat Protoc.* **2013**, *8*, 131−147.
(27) Schmidt, M. J.; Fedoseev, A.; Summerer, D.; Drescher, M. Genetically Encoded Spin Labels for in Vitro and in-Cell EPR Studies of Native Proteins. In *Methods in Enzymology*; Qin, P. Z.; Warncke, K., Eds.; Academic Press: 2015; Chapter 18, Vol. *563*, pp 483−502.
(28) Azarkh, M.; Okle, O.; Singh, V.; Seemann, I. T.; Hartig, J. S.; Dietrich, D. R.; Drescher, M. Long-range distance determination in a DNA model system inside Xenopus laevis oocytes by in-cell spin-label EPR. *ChemBioChem* **2011**, *12*, 1992−1995.
(29) Krstić, I.; Hänsel, R.; Romainczyk, O.; Engels, J. W.; Dötsch, V.; Prisner, T. F. Long-range distance measurements on nucleic acids in cells by pulsed EPR spectroscopy. *Angew. Chem., Int. Ed.* **2011**, *50*, 5070−5074.
(30) Joseph, B.; Sikora, A.; Cafiso, D. S. Ligand induced conformational changes of a membrane transporter in E. coli cells observed with DEER/PELDOR. *J. Am. Chem. Soc.* **2016**, *138*, 1844−1847.
(31) Lu, Y.; Yeung, N.; Sieracki, N.; Marshall, N. M. Design of functional metalloproteins. *Nature* **2009**, *460*, 855−862.
(32) Denysenkov, V. P.; Prisner, T. F.; Stubbe, J.; Bennati, M. High-field pulsed electron−electron double resonance spectroscopy to determine the orientation of the tyrosyl radicals in ribonucleotide reductase. *Proc. Natl. Acad. Sci. U.S.A.* **2006**, *103*, 13386.
(33) Qi, M.; Groß, A.; Jeschke, G.; Godt, A.; Drescher, M. Gd(III)-PyMTA label is suitable for in-cell EPR. *J. Am. Chem. Soc.* **2014**, *136*, 15366−15378.
(34) Yang, Y.; Yang, F.; Gong, Y.-J.; Chen, J.-L.; Goldfarb, D.; Su, X.-C. A reactive, rigid GdIII labeling tag for in-cell EPR distance measurements in proteins. *Angew. Chem., Int. Ed.* **2017**, *56*, 2914−2918.
(35) Martorana, A.; Bellapadrona, G.; Feintuch, A.; Di Gregorio, E.; Aime, S.; Goldfarb, D. Probing protein conformation in cells by EPR distance measurements using Gd3+ spin labeling. *J. Am. Chem. Soc.* **2014**, *136*, 13458−13465.
(36) Jassoy, J. J.; Berndhäuser, A.; Duthie, F.; Kühn, S. P.; Hagelueken, G.; Schiemann, O. Versatile Trityl Spin Labels for Nanometer Distance Measurements on Biomolecules In Vitro and within Cells. *Angew. Chem., Int. Ed.* **2017**, *56*, 177−181.
(37) Cattani, J.; Subramaniam, V.; Drescher, M. Room-temperature in-cell EPR spectroscopy: Alpha-synuclein disease variants remain intrinsically disordered in the cell. *Phys. Chem. Chem. Phys.* **2017**, *19*, 18147−18151.
(38) Robotta, M.; Gerding, H. R.; Vogel, A.; Hauser, K.; Schildknecht, S.; Karreman, C.; Leist, M.; Subramaniam, V.; Drescher, M. Alpha-synuclein binds to the inner membrane of mitochondria in an α-helical conformation. *ChemBioChem* **2014**, *15*, 2499−2502.
(39) Bobko, A. A.; Kirilyuk, I. A.; Grigor'ev, I. A.; Zweier, J. L.; Khramtsov, V. V. Reversible reduction of nitroxides to hydroxylamines: Roles for ascorbate and glutathione. *Free Radic. Biol. Med.* **2007**, *42*, 404−412.
(40) Jagtap, A. P.; Krstic, I.; Kunjir, N. C.; Hänsel, R.; Prisner, T. F.; Sigurdsson, S. T. Sterically shielded spin labels for in-cell EPR spectroscopy: Analysis of stability in reducing environment. *Free Radical Res.* **2015**, *49*, 78−85.
(41) Karthikeyan, G.; Bonucci, A.; Casano, G.; Gerbaud, G.; Abel, S.; Thomé, V.; Kodjabachian, L.; Magalon, A.; Guigliarelli, B.; Belle, V.; Ouari, O.; Mileo, E. A bioresistant nitroxide spin label for in-cell EPR spectroscopy: In vitro and in oocytes protein structural dynamics studies. *Angew. Chem.* **2018**, *130*, 1380−1384.
(42) Saha, S.; Jagtap, A. P.; Sigurdsson, S. T. Site-directed spin labeling of 2′-amino groups in RNA with isoindoline nitroxides that are resistant to reduction. *Chem. Commun.* **2015**, *51*, 13142−13145.
(43) Yang, Y.; Yang, F.; Li, X.-Y.; Su, X.-C.; Goldfarb, D. In-cell EPR distance measurements on ubiquitin labeled with a rigid PyMTA-Gd(III) tag. *J. Phys. Chem. B* **2019**, *123*, 1050−1059.
(44) Barhate, N.; Cekan, P.; Massey, A. P.; Sigurdsson, S. T. A nucleoside that contains a rigid nitroxide spin label: A fluorophore in disguise. *Angew. Chem., Int. Ed.* **2007**, *46*, 2655−2658.
(45) Höbartner, C.; Sicoli, G.; Wachowius, F.; Gophane, D. B.; Sigurdsson, S. T. Synthesis and characterization of RNA containing a rigid and nonperturbing cytidine-derived spin label. *J. Org. Chem.* **2012**, *77*, 7749−7754.
(46) Grytz, C. M.; Kazemi, S.; Marko, A.; Cekan, P.; Güntert, P.; Sigurdsson, S. T.; Prisner, T. F. Determination of helix orientations in a flexible DNA by multi-frequency EPR spectroscopy. *Phys. Chem. Chem. Phys.* **2017**, *19*, 29801−29811.
(47) Haugland, M. M.; El-Sagheer, A. H.; Porter, R. J.; Peña, J.; Brown, T.; Anderson, E. A.; Lovett, J. E. 2′-Alkynylnucleotides: A sequence- and spin label-flexible strategy for EPR spectroscopy in DNA. *J. Am. Chem. Soc.* **2016**, *138*, 9069−9072.
(48) Gophane, D. B.; Sigurdsson, S. T. Hydrogen-bonding controlled rigidity of an isoindoline-derived nitroxide spin label for nucleic acids. *Chem. Commun.* **2013**, *49*, 999−1001.
(49) Lin, K.-Y.; Jones, R. J.; Matteucci, M. Tricyclic 2′-deoxycytidine analogs: Syntheses and incorporation into oligodeoxynucleotides which have enhanced binding to complementary RNA. *J. Am. Chem. Soc.* **1995**, *117*, 3873−3874.
(50) Volodarsky, L. B.; Reznikov, V. A.; Ovcharenko, V. I. *Synthetic Chemistry of Stable Nitroxides*; Taylor & Francis, 1993.
(51) Cekan, P.; Smith, A. L.; Barhate, N.; Robinson, B. H.; Sigurdsson, S. T. Rigid spin-labeled nucleoside Ç: A nonperturbing

EPR probe of nucleic acid conformation. *Nucleic Acids Res.* **2008**, *36*, 5946−5954.
(52) Juliusson, H. Y.; Segler, A.-L. J.; Sigurdsson, S. T. Benzoyl-protected hydroxylamines for improved chemical synthesis of oligonucleotides containing nitroxide spin labels. *Eur. J. Org. Chem.* **2019**, *2019*, 3799−3805.
(53) Hatano, A.; Terado, N.; Kanno, Y.; Nakamura, T.; Kawai, G. Synthesis of a protected ribonucleoside phosphoramidite-linked spin label via an alkynyl chain at the 5′ position of uridine. *Synth. Commun.* **2019**, *49*, 136−145.
(54) Sen, V. D.; Golubev, V. A. Kinetics and mechanism for acid-catalyzed disproportionation of 2,2,6,6-tetramethylpiperidine-1-oxyl. *J. Phys. Org. Chem.* **2009**, *22*, 138−143.
(55) Cekan, P.; Sigurdsson, S. T. Single base interrogation by a fluorescent nucleotide: each of the four DNA bases identified by fluorescence spectroscopy. *Chem. Commun.* **2008**, 3393−3395.
(56) Weinrich, T.; Gränz, M.; Grünewald, C.; Prisner, T. F.; Göbel, M. W. Synthesis of a Cytidine Phosphoramidite with Protected Nitroxide Spin Label for EPR Experiments with RNA. *Eur. J. Org. Chem.* **2017**, *2017*, 491−496.
(57) Engman, K. C.; Sandin, P.; Osborne, S.; Brown, T.; Billeter, M.; Lincoln, P.; Nordén, B.; Albinsson, B.; Wilhelmsson, L. M. DNA adopts normal B-form upon incorporation of highly fluorescent DNA base analogue tC: NMR structure and UV-Vis spectroscopy characterization. *Nucleic Acids Res.* **2004**, *32*, 5087−5095.
(58) Sandin, P.; Stengel, G.; Ljungdahl, T.; Börjesson, K.; Macao, B.; Wilhelmsson, L. M. Highly efficient incorporation of the fluorescent nucleotide analogs tC and tCO by Klenow fragment. *Nucleic Acids Res.* **2009**, *37*, 3924−3933.

https://dx.doi.org/10.1021/acs.joc.9b02988
J. Org. Chem. 2020, 85, 4036−4046